

Quantitative Analysis of Intermolecular Interactions in the Crystal Structure of 4-(2-(ethoxymethyl)phenyl)-1H-pyrazol-3-ol

Rahul Shukla¹,
Chetan Shripanavar²,
Deepak Chopra²,
Bubbly SG³ and
SB Gudennavar³

Abstract

A quantitative analysis of the intermolecular interactions in the crystal structure of a pyrazole derivative namely 4-(2-(ethoxymethyl) phenyl)-1H-pyrazol-3-ol has been performed. The compound crystallizes with one molecule in the asymmetric unit in the monoclinic centrosymmetric space group $P2_1/n$. SCXRD studies revealed the presence of O-H...N, N-H...O H-bonds along with C-H...O, C-H... π and H...H interactions in the crystal. The molecular electrostatic map clearly demonstrates the nature of different atoms within the molecule. The lattice energy of the compound was calculated using PIXEL. The decomposition of the interaction energies obtained for different molecular pairs clearly demonstrated that the nature and strength of interactions present in a given molecular pair was directly correlated with the strength of the donor or/and acceptor atom present in the molecule.

Keywords: Lattice energy; Crystal structure; Pyrazole

Received: August 05, 2015; **Accepted:** September 16, 2015; **Published:** September 21, 2015

Introduction

Studying intermolecular interactions in molecular crystals has been a very important aspect of supramolecular chemistry [1-3]. Both strong and weak intermolecular interactions have been observed to be responsible for the 3D arrangement of molecules in a crystal [4-6] and hence a detailed analysis of their nature is very important. Strong intermolecular interactions such as N-H...O/N, O-H...O/N [7-9] has been well studied and documented in the literature. In the past 15-20 years, in addition to strong interactions, weak interactions such as C-H...O/N [10,11], C-H...X (X=F, -Cl, -Br, -I) [12-17], C-H... π [18,19], I π ... π [20,21], X...X (X=F, Cl, Br, I) [22-25] has garnered attention across the world. Apart from this, various studies have also been performed to understand the interplay between strong and weak interactions within the same molecule in the crystal [26-28]. Along with experimental analysis, detailed computational studies have also become an important tool in delineating the strength and nature of intermolecular interactions [12,29-31].

In our study, we have performed a complete structural analysis on a pyrazole derivative, namely 4-(2-(ethoxymethyl) phenyl)-1H-pyrazol-3-ol (PRZ). Pyrazoles are five membered heterocyclic molecules with two nitrogens adjacent to each other. These are

- 1 Crystallography and Crystal Chemistry Laboratory, Department of Chemistry, Indian Institute of Science Education and Research, Bhopal, Madhya Pradesh, India
- 2 Department of Agrochemicals and Pest Management, Devchand College, Arjunnagar, Karnataka, India
- 3 Department of Physics, Christ University, Bengaluru, Karnataka, India

Corresponding author: Deepak Chopra

✉ dchopra@iiserb.ac.in

Crystallography and Crystal Chemistry Laboratory, Department of Chemistry, Indian Institute of Science Education and Research, Bhopal, Madhya Pradesh, India.

Fax: 91-755-6692392

Citation: Shukla R, Shripanavar C, Chopra D, et al. Quantitative Analysis of Intermolecular Interactions in the Crystal Structure of 4-(2-(ethoxymethyl)phenyl)-1H-pyrazol-3-ol. Struct Chem Crystallogr Commun. 2015, 1:1.

aromatic systems with six delocalized π electrons. It has been observed that pyrazole derivatives are biologically important with applications in antimicrobial [32], analgesic [33], anti-cancer activities [34] and hence it is important to understand the molecular conformation and intermolecular interactions in pyrazole derivatives. In PRZ, we have two nitrogen atoms and two oxygen atoms in different electronic environments which can participate in hydrogen bonding. Apart from this, PRZ have C-H bonds which can act as weak hydrogen bond donors. The π rings present in the molecule can also participate in the formation of intermolecular interactions and can play a role in crystal packing. Due to the above-mentioned properties, it was of interest to study the nature and strength of intermolecular interactions in PRZ.

Synthesis of PRZ

0.190 g (0.1 mol) of 4-(2-(hydroxymethyl) phenyl)-1H-pyrazol-3-ol, was dissolved in 10 ml ethanol and 2 drops of H_2SO_4 . The reaction mixture was refluxed for 6 hr at 80°C temperature and cooled to separate out the final product PRZ. The compound is recrystallized by dissolving it in ethanol. By the process of slow evaporation colorless crystals of the product were obtained. The scheme of the reaction is as shown in (Figure 1).

Crystal growth and single-crystal X-ray diffraction

Suitable crystals for X-ray diffraction studies were grown in ethanol at room temperature through solvent evaporation method. White transparent single crystals were obtained. Single crystal X-ray measurements were carried out on a Bruker AXS Kappa Apex 2 CCD diffractometer using monochromated $MoK\alpha$ radiation ($\lambda=0.71073 \text{ \AA}$) in phi (ϕ) and omega (ω) scans at 292(2) K. Unit cell measurement, data collection, integration, scaling and absorption corrections were performed using Bruker Apex II software [35]. The intensity data were processed by using the Bruker SAINT [36] suite of programs. The crystal structure was refined by the full matrix least squares method using SHELXL14 [37] present in the program suite WinGX [38]. Empirical absorption correction was applied using SADABS [39]. The non-hydrogen atoms were refined anisotropically and the hydrogen atoms bonded to C and N atoms were positioned geometrically and refined using a riding model with $U_{iso}(H)=1.2U_{eq}(C, N)$. The molecular connectivity and the crystal packing diagrams were generated using the Mercury 3.1 (CCDC) program [40]. Geometrical calculations were done using PARST [41] and PLATON [42]. The details of data collection and crystal structure refinement are shown in (Table 1).

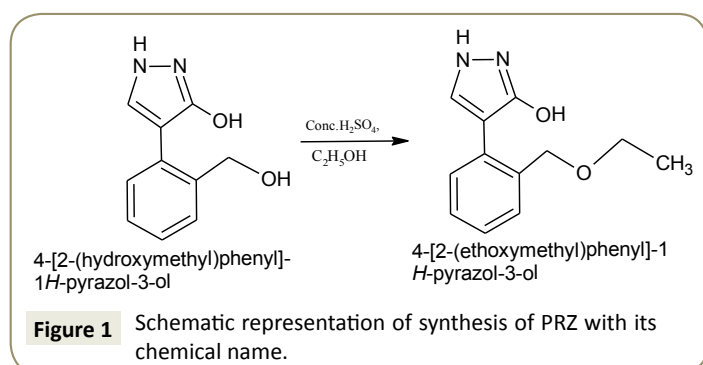
Theoretical calculations

Optimization of the crystal structure was performed at MP2 level of theory at 6-311G** basis set using Gaussian09 [43]. The minima of the optimized structure were confirmed by the absence of imaginary frequencies. All calculations for the analysis of the crystal structure and intermolecular interactions were performed at the crystal geometry. The C-H bond length was moved to its neutron value of 1.08 Å while O-H and N-H bond was fixed at 1.00 Å. The molecular electrostatic potential were plotted on a Hirshfeld iso-surface using Crystal Explorer 3.1 [44] at 6-311G** basis set with wave functions generated using TONTO [45]. Lattice energy and intermolecular interaction energies were calculated using PIXEL code present in the CLP computer program [31]. The program PIXEL provides the advantage of partitioning the total

Table 1 Single crystal data collection and refinement details of PRZ.

Sample Code	PRZ
Formula	$C_{12}H_{14}N_2O_2$
Formula Weight	218.15
Temperature/ K	292 (2) K
Wavelength (Å)	0.71073
Solvent System	Ethanol (RT)
CCDC number	1415498
Crystal system	Monoclinic
Space group	$P2_1/n$
a (Å)	9.1554 (13)
b (Å)	7.0628 (8)
c (Å)	17.784 (3)
α (°)	90
β (°)	94.371 (4)
γ (°)	90
V (Å ³)	1146.6 (3)
Z	4
μ (mm ⁻¹)	0.088
F(000)	464
θ (min, max)	2.297, 25.734
Treatment of hydrogens	Fixed
$h_{min,max}$ $k_{min,max}$ $l_{min,max}$	-11, 11, -8, 8, -21, 21
No. of ref.	12302
No. of unique ref./obs. ref.	2181 / 1642
No. parameters	174
R_{all} R_{obs}	0.0683, 0.0461
wR_{2all} wR_{2obs}	0.1118, 0.0995
$\Delta\rho_{min,max}$ (e Å ⁻³)	-0.150, 0.171
G. O. F.	1.044

interaction energy for the different molecular pair's into the corresponding coulombic, polarization, dispersion and repulsion components respectively. Coulombic terms are handled by Coulomb's law while the polarization terms are calculated utilizing the linear dipole approximation in PIXEL, where the incoming electric field acts on local polarizabilities and generates a dipole with its associated dipole separation energy. The treatment of the dispersion terms are simulated in London's inverse sixth power approximation, involving ionization potentials and polarizabilities and the repulsion is represented as a modulated function of wave function overlap. Some selected molecular pairs were further analyzed by using AIMALL [46] which is based on Bader's theory of atoms in molecules [47]. It gives us properties like ρ , $\nabla^2\rho$, local potential energy (V_b), and kinetic potential energy (G_b) at the bond critical point [44]. For AIMALL, *ab initio* calculations for all the molecular pairs were performed at the MP2/6-311G** level of theory (with "density = current" keyword) using Gaussian 09. Then the formatted checkpoint file (fchk) was considered as the input for AIMALL, which is then used to generate the wave function file (.wfx file) by the software itself and followed by the topological analysis. Contributions from different interactions were also analyzed by fingerprint plot [49] generated using Crystal Explorer 3.1.



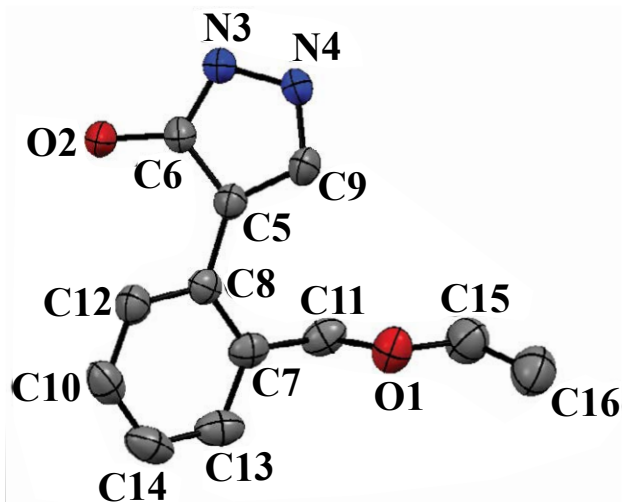


Figure 2 ORTEP of PRZ at 50% ellipsoidal probability along with the atom numbering. Hydrogen atoms omitted for clarity.

Results and Discussion

The ORTEP of PRZ has been shown in (Figure 2). PRZ crystallized in a monoclinic system in $P2_1/n$ space group with $Z = 4$. The molecule can be broadly divided into two different parts. The first was the pyrazol-3-ol and the second is the phenyl group to which a flexible ethoxymethyl group is attached. A superimposition of the structure of PRZ obtained from the crystal geometry and the optimized geometry has been shown in (Figure 3). Torsion I and II values showed that the geometry of the pyrazole group connected to the phenyl ring is nearly equal to each other. The major difference was observed in the flexible ethoxy methyl group where the experimental value for Torsion III was $97.30(2)^\circ$ while that obtained from the theoretical calculation was 85.31° (Table 2).

The lattice energy of the molecule was calculated to be -162.2 kJ/mol (Table 3). Energy partitioning showed that the maximum contribution towards the lattice stabilization is coming from the coulombic and dispersion component with each contribution around 40% while the remaining contribution comes from the polarization energy.

The molecular electrostatic potential map was plotted on Hirshfeld iso surface with electrostatic potential ranging from 0.05 a.u. (blue) to -0.05 (red). The molecular electrostatic potential (MEP) map of PRZ revealed that the regions of negative potential are concentrated around the electronegative oxygen and nitrogen atom present in the molecule (Figure 4). The region around the hydrogen atom and C-H bond of the ethoxy methyl group constituted the positive region in the molecule. The π system present in the molecule also exhibited a negative potential but as clearly visible from the MEP plot the magnitude of the potential is less as compared to those observed for the oxygen and nitrogen atoms.

Different intermolecular interactions present in PRZ along with geometrical parameters, symmetry and interaction energies partitioned into different energy components has been

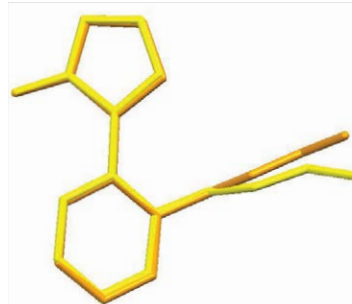


Figure 3 Structural overlay diagram of PRZ at crystal geometry (in yellow) with that of the optimized geometry (in orange).

Table 2 Experimental and theoretical values obtained for selected torsion angles in PRZ.

S. No.	Torsion	Experimental Value	Theoretical Value
I	C9-C5-C6-C7	$45.26^\circ(3)$	42.55°
II	C9-C5-C8-C12	$136.01^\circ(2)$	137.49°
III	C8-C7-C11-O1	$97.30^\circ(2)$	85.31°

Table 3 Lattice energy of PRZ partitioned into different energy components.

Code	E_{coul} (kJ/mol)	E_{pol} (kJ/mol)	E_{disp} (kJ/mol)	E_{rep} (kJ/mol)	E_{tot} (kJ/mol)
PRZ	-138.4	-72.7	-136.9	185.8	-162.2

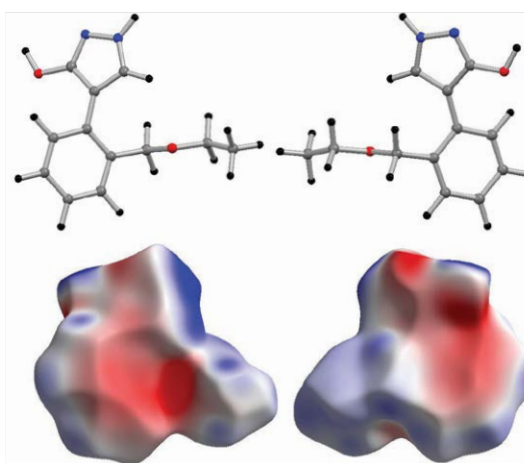


Figure 4 MEP plotted on the Hirshfeld iso surface of PRZ. The ranges of ESP are from 0.05 a.u. (blue) to -0.05 a.u. (red).

represented in (Table 4). The packing diagram of PRZ down the bc plane is shown in (Figure 5). The most stabilized molecular pair was observed to be a short O-H...N H-bond along the c -axis having H...N distance of 1.71 \AA and O-H...N angle being 171° (I). The stabilization energy was calculated to be -69.7 kJ/mol. The stability of this molecular pair is driven by the coulombic contribution ($\sim 56\%$), followed by polarization ($\sim 33\%$) and dispersion ($\sim 11\%$) components respectively (Table 4). The second most stabilized molecular pair also contained a short N-H...O H-bond along with the presence of C-H... π interactions. The interaction energy for this molecular pair was calculated to be -56.6 kJ/mol. In this molecular pair, the contribution of the

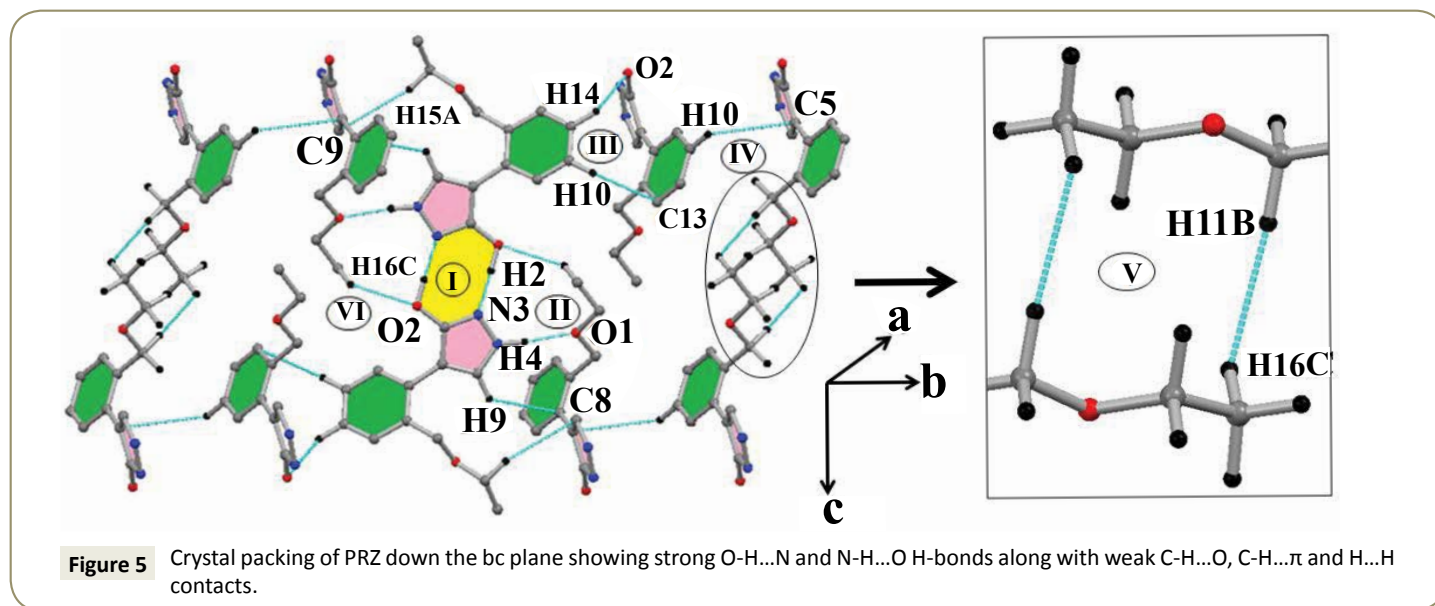


Table 4 List of intermolecular interaction energies (kJ/mol) present in PRZ.

Molecular Pairs	Interactions	X...A (Å)	D-X...A (°)	Symmetry Code	Centroid-Centroid Dist. (Å)	E_{coul} (kJ/mol)	E_{pol} (kJ/mol)	E_{disp} (kJ/mol)	E_{rep} (kJ/mol)	E_{tot} (kJ/mol)
I	O2-H2...N3	1.71	176	1-x,-y,-z+1	9.239	-153.0	-88.9	-30.8	203.1	-69.7
II	N4-H4...O1	1.95	172	0.5-x,-0.5+y, 0.5-z	5.274	-40.6	-17.3	-45.6	46.8	-56.6
	C9-H9...C8(π)	2.90	129							
III	C15-H15A...C9(π)	3.03	160	1.5-x, 0.5+y, 0.5-z	6.320	-6.6	-3.0	-24.1	13.6	-20.1
	C10-H10...C13(π)	2.90	131							
IV	C14-H14...O2	2.71	128	x,-1+y,z	7.063	-5.9	-2.2	-21.1	11.6	-17.6
	C10-H10...C5(π)	3.27	136							
V	C11-H11B...H16C	2.40	175	-x+1,-y,-z	9.079	-2.9	-1.8	-20.9	11.2	-14.3
	em...em	-	-							
VI	C16-H16C...O2	2.61	134	-0.5+x,0.5-y,-0.5+z	9.787	-4.6	-1.1	-8.6	5.1	-9.3

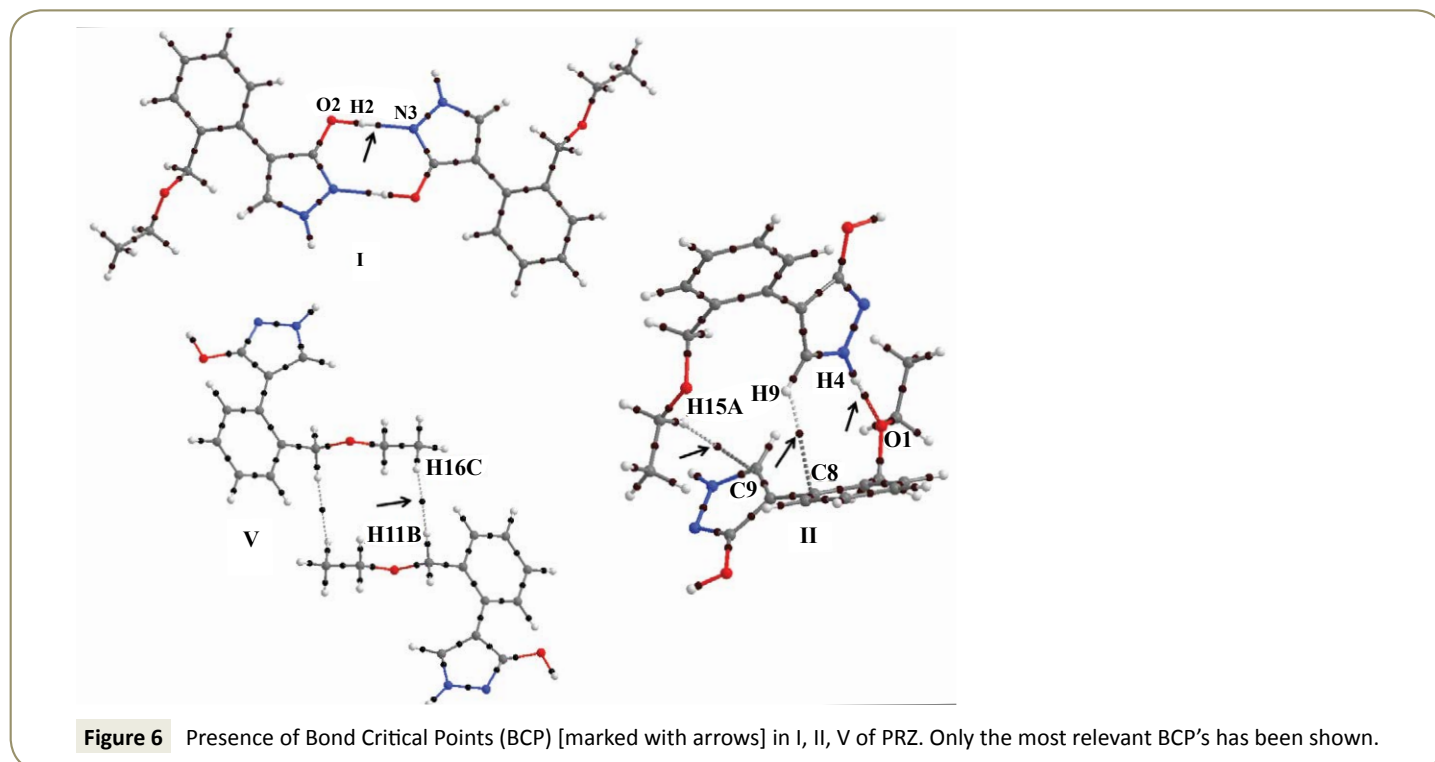
dispersion component was observed to be greater than that of the polarization component. The reason for the increased contribution from the dispersion component can be attributed to the presence of weak C-H... π interactions which are of a dispersive nature (**Figure 5**). Motif III consisted of two weak interactions. The first was a weak C-H...O interaction and the other being a C-H... π interaction. This molecular pair was of a dispersive nature with the dispersion component dominating with 71.5% contribution towards the total stabilization (**Table 4**). Motif-IV has stabilization energy of -17.6 kJ/mol because of the presence of a weak C-H...O interaction. As observed for the previous molecular pairs with weak interactions, also in the current case, the stability was governed by dispersion component (~72%) followed by coulombic (~20%) and polarization (~8%) contribution. Motif-V represents a unique molecular pair with the presence of short and highly directional H...H contacts (**Table 4**). The crystal packing

clearly depicts the presence of side chain interactions involving the ethoxy methyl (em) group of one molecule with a similar group of a centrosymmetrically related molecule and this leads to the formation of a molecular pair which can be best described as arising from purely dispersive forces (**Figure 5**). The dispersive nature is clearly evident from the decomposition of the energy component indicating a contribution of ~82% towards the total stabilization (**Table 4**). The least stabilized molecular pair consists of a C-H...O interaction, the interaction energy being -9.3 kJ/mol.

QTAIM analysis using AIMALL was performed on motif I and II which contains strong hydrogen bonds and on motif V which contained a short H...H contact. (**Table 5**) shows the topological parameters obtained from the analysis and (**Figure 6**) shows the Bond Critical Point (BCP) obtained between the interacting atoms marked with arrow in (**Figure 6**). The ρ value for H...N contact was $0.340 \text{ e}/\text{\AA}^3$ while for H...O interaction was observed to be $0.163 \text{ e}/\text{\AA}^3$.

Table 5 Topological parameters at BCP for I, II, V in PRZ.

Motif	Interaction	Bond Path Length (BCP) (Å)	ρ ($e / \text{Å}^3$)	$\nabla^2\rho$ ($e / \text{Å}^5$)	$IV_b I / G_b$
I	H2...N3	1.733	0.340	2.721	0.998
II	H4...O1	1.970	0.163	2.235	0.908
III	H9...C8	3.193	0.040	0.401	0.819
IV	H15A...C9	3.279	0.031	0.309	0.871
V	H11B...H16C	2.464	0.035	0.367	0.846



Similarly the $\nabla^2\rho$ for H...N interaction was higher than that of H...O contact. For motif II, a BCP was also observed between hydrogen and carbon atom confirming the presence of a C-H... π interaction. In V, multiple bcp were observed between hydrogen atoms further establishing the significance of H...H contacts. The most relevant BCP in V was between H11B and H16C with ρ and $\nabla^2\rho$ values of $0.035e/\text{Å}^3$ and $0.367e/\text{Å}^5$ respectively. The obtained value is similar to values reported previously for H...H interactions [50]. As expected, the magnitude of ρ and $\nabla^2\rho$ clearly depicts that the strength of H...H interactions is much lower relative to strong hydrogen bonds.

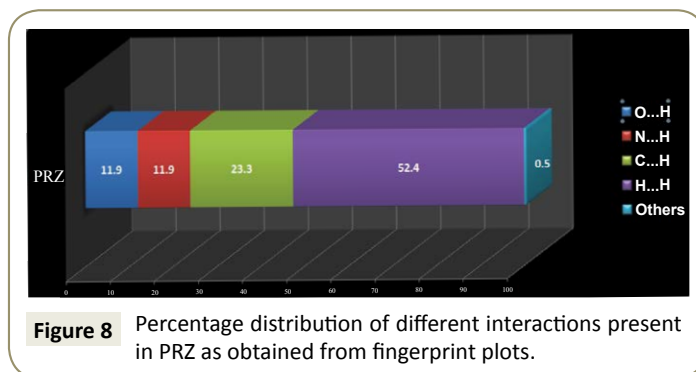
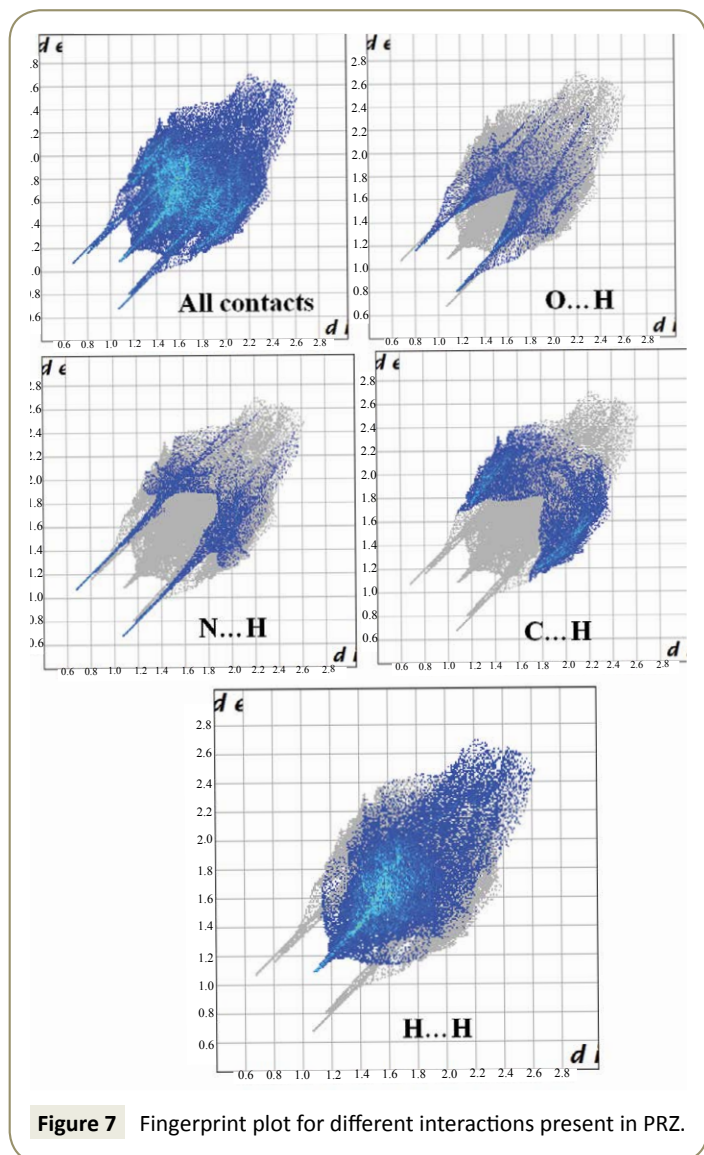
We have further analyzed the crystal structure of PRZ by looking at the fingerprint plot for different interactions (**Figure 7**). Fingerprint plot is a unique tool to represent the intermolecular interactions present in the crystal structure. The maximum contribution in the fingerprint plot is from H...H contacts (52.4%). This high contribution can be attributed to the presence of ethoxy methyl group in the molecule which involves the existence of dispersion interactions as discussed earlier. The next contribution is from C...H contacts (23.3%) on account of the presence of C-H... π interactions. N...H and O...H contributed equally to the extent of 19.3% (**Figure 8**).

Conclusion

In this study, we have quantitatively analyzed the intermolecular interactions present in the crystal structure of 4-(2-(ethoxymethyl) phenyl)-1H-pyrazol-3-ol. The geometry of the crystal structure is largely similar to the optimized geometry with slight deviation in the flexible ethoxy methyl region. Coulombic and dispersion energies both have nearly equal contributions towards the stabilization of the crystal lattice. Calculations on the intermolecular interaction energies showed that in case of strong H-bonds such as N-H...O or O-H...N, coulombic contribution played a dominating role but in presence of the weak interactions, dispersion becomes a dominating factor. This study can help us in designing different biologically active derivatives of pyrazoles by changing the strength of donor and/or acceptor atom which can give rise to interactions of different strength and nature which in turn can help in identifying binding capabilities of such molecules with enzymes. Due to the biological activity of pyrazole derivatives, polymorphism studies on PRZ will be of interest with regard to pharmaceutical industry.

Acknowledgements

RS thanks DST for INSPIRE-PhD fellowship. DC thanks IISERB for providing infrastructure and research facilities.



References

- Bombicz P, Gruber T, Fischer C, Weber E, Kálmán A (2014) Fine tuning of crystal architecture by intermolecular interactions: synthon engineering. *Cryst Eng Comm* 16: 3646-3654.
- Desiraju GR (2000) Hydrogen bonds and other intermolecular interactions in organometallic crystals. *J Chem Soc Dalton Trans*: 3745-3751.
- Tumer MJ, Grabowsky S, Jayatalika D, Spackman MA (2014) Accurate and Efficient Model Energies for Exploring Intermolecular Interactions in Molecular Crystals. *J Phys Chem Lett* 5: 4249-4255.
- Perumalla SR, Sun CC (2013) Synthon preference in O-protonated amide crystals – dominance of short strong hydrogen bonds. *Cryst Eng Comm* 15: 8941-8946.
- Dey D, Chopra D (2015) N–H... π induced configurational isomerism and the role of temperature in the Z to E isomerization of 2-fluoro-N'-(3-fluorophenyl)benzimidamide. *Cryst Eng Comm* 17: 5288-5298.
- Wang L, Hu Y, Wang W, Liu F, Huang K (2014) Energetic multi-component molecular solids of tetrafluoroterephthalic acid with some aza compounds by strong hydrogen bonds and weak intermolecular interactions of C–H...F and C–H...O. *Cryst Eng Comm* 16: 4142-4161.
- Aniota M, Dega-Szafran Z, Katrusiak A, Szafran M (2014) NH...O and OH...O interactions of glycine derivatives with squaric acid. *New J Chem* 38: 355-3568.
- Vishnupriya R, Suresh J, Sivakumar S, Kumar RR (2013) N-H...O and N-H...N interactions in three pyran derivatives. *Acta Cryst C* 69: 642-646.
- Najdian A, Shakourian-Fard M, Fattahi A (2014) Cooperativity effects of intramolecular OH...O interactions on pKa values of polyolalkyl sulfonic acids in the gas phase and solution: a density functional theory study. *J Phys Org Chem* 27: 604-612.
- Wiberg KB, Lambert KM, Bailey WF (2015) The Role of CH...O Coulombic Interactions in Determining Rotameric Conformations of Phenyl Substituted 1,3-Dioxanes and Tetrahydropyrans. *J Org Chem* 80: 7884-7889.
- Brovarets OO, Yurenko YP, Hovorun DM (2013) Intermolecular CH...O/N H-bonds in the biologically important pairs of natural nucleobases: a thorough quantum-chemical study. *J Biomol Struct Dyn* 32: 993-1022.
- Shukla R, Chopra D (2015) Crystallographic and computational investigation of intermolecular interactions involving organic fluorine with relevance to the hybridization of the carbon atom. *Cryst Eng Comm* 17: 3596-3609.
- Hathwar VR, Roopan SM, Subhashini R, Khan FN, Row TNG (2010) Analysis of Cl...Cl and C–H...Cl intermolecular interactions involving chlorine in substituted 2-chloroquinoline derivatives. *J Chem Sci* 122: 677-685.
- Elahi A, Kant R (2014) Contribution of weak intermolecular interactions in 3-acetyl coumarin derivatives. *Eur Chem Bull* 3: 763-769.
- Trzybiński D, Sikorski A (2013) Solvent-bridged frameworks of hydrogen bonds in crystals of 9-aminoacridinium halides. *Cryst Eng Comm* 15: 6808-6818.
- Hathwar VR, Chopra D, Panini P, Row TNG (2014) Revealing the polarizability of organic fluorine in the trifluoromethyl group: Implications in supramolecular chemistry. *Cryst Growth Des* 14: 5366-5369.
- Panini P, Venugopal KN, Odhav B, Chopra D (2014) Polymorphism in two biologically active dihydropyrimidinium hydrochloride derivatives: quantitative inputs towards the energetics associated with crystal packing. *Acta Cryst B* 70: 681-696.
- Nishio M, Umezawa Y, Honda K, Tsuboyama S, Suezawa H (2009) CH/ π hydrogen bonds in organic and organometallic chemistry. *Cryst Eng Comm* 11: 1757-1788.
- Nishio M (2011) The CH/ π hydrogen bond in chemistry. Conformation, supramolecules, optical resolution and interactions involving carbohydrates. *Phys Chem Chem Phys* 13: 13873-13900.
- Shukla R, Mohan TP, Vishalakshi B, Chopra D (2014) Experimental and theoretical analysis of Ip... π intermolecular interactions in derivatives of 1,2,4-triazoles. *Cryst Eng Comm* 16: 1702-1713.
- Elgi M, Sarkhel S (2007) Lone Pair-Aromatic Interactions: To Stabilize or Not to Stabilize. *Acc Chem Res* 40: 197-205.
- Pérez-Torrallba M, García MÁ, López C, Toralba MC, Torres MR, et al. (2014) Structural Investigation of Weak Intermolecular Interactions (Hydrogen and Halogen Bonds) in Fluorine-Substituted Benzimidazoles. *Cryst Growth Des* 14: 3499-3509.
- Nayak SK, Reddy MK, Row TNG, Chopra D (2011) Role of Hetero-Halogen (F...X, X = Cl, Br, and I) or Homo-Halogen (X...X, X = F, Cl, Br, and I) Interactions in Substituted Benzanilides. *Cryst Growth Des* 11: 1578-1596.
- Metrangolo P, Resnati G (2014) Type II halogen...halogen contacts are halogen bonds. *IUCr* 1: 5-7.
- Politzer P, Murray JS, Clark T (2013) Halogen bonding and other s-hole interactions: a perspective. *Phys Chem Chem Phys* 15: 11178-11189.
- Panini P, Chopra D (2012) Role of intermolecular interactions involving organic fluorine in trifluoromethylated benzanilides. *Cryst Eng Comm* 14: 1972-1989.
- Panini P, Chopra D (2013) Quantitative insights into energy contributions of intermolecular interactions in fluorine and trifluoromethyl substituted isomeric N-phenylacetamides and N-methylbenzamides. *Cryst Eng Comm* 15: 3711-3733.
- Dey D, Mohan TP, Vishalakshi B, Chopra D (2014) Computational Study of the Formation of Short Centrosymmetric N–H...S Supramolecular Synthon and Related Weak Interactions in Crystalline 1,2,4-Triazoles. *Cryst Growth Des* 14: 5881-5896.
- Esrifili MD, Ahmadi B (2012) A theoretical investigation on the nature of Cl...N and Br...N halogen bonds in F-Ar-X...NCY complexes (X = Cl, Br and Y = H, F, Cl, Br, OH, NH₂, CH₃ and CN). *Comp Theor Chem* 997: 77-82.
- Dunitz JD, Gavezzotti A, Rizzato S (2014) "Coulombic compression", a pervasive force in ionic solids. A study of anion stacking in croconate crystals. *Cryst Growth Des* 14: 357-366.
- Dunitz JD, Gavezzotti A (2012) Supramolecular synthons: validation and ranking of intermolecular interaction energies. *Cryst Growth Des* 12: 5873-5877.
- Sharshira EM, Hamada NMM (2012) Synthesis and Antimicrobial Evaluation of Some Pyrazole Derivatives. *Molecules* 17: 4962-4971.
- Saad HA, Osman NA, Moustafa AH (2011) Synthesis and Analgesic Activity of Some New Pyrazoles and Triazoles Bearing a 6,8-Dibromo-2-methylquinazoline Moiety. *Molecules* 16: 10187-10201.
- Balbi A, Anzaldi M, Macció C, Aiello C, Mazzei M, Gangemi R (2011) Synthesis and biological evaluation of novel pyrazole derivatives with anticancer activity. *Eur J Med Chem* 46: 5293-5309.

- 35 Apex2, Version 2 User Manual, M86-E01078, Bruker Analytical X-ray Systems, Madison, WI, 2006.
- 36 Siemens, SMART System, Siemens Analytical X-ray Instruments Inc., Madison, MI, 1995.
- 37 Sheldrick GM (2008) A short of SHELX. *Acta Crystallogr Sect. A: Found Crystallogr* 64: 112-122.
- 38 Farrugia LJ (1999) WinGX suite for small-molecule single-crystal crystallography. *J Appl Crystallogr* 32: 837-838.
- 39 Sheldrick GM (2007) SADABS, Bruker AXS, Inc. Madison, WI.
- 40 Macrae CF, Bruno IJ, Chisholm JA, Edgington PR, McCabe P, et al. (2008) Mercury CSD 2.0 - New Features for the Visualization and Investigation of Crystal Structures. *J Appl Cryst* 41: 466-470.
- 41 Nardelli M (1995) PARST95-an update to PARST: a system of Fortran routines for calculating molecular structure parameters from the results of crystal structure analyses. *J Appl Cryst* 28: 659-659.
- 42 Spek AL (2009) Structure validation in chemical crystallography. *Acta Cryst D* 65: 148-155.
- 43 Gaussian 09, Revision D.01, Frisch M J, Trucks G W, Schlegel H B, Scuseria G E, Robb M A, Cheeseman J R, Scalmani G, Barone V, Mennucci B, Petersson G A, Nakatsuji H, Caricato M, Li X, Hratchian H P, Izmaylov A F, Bloino J, Zheng G, Sonnenberg J L, Hada M, Ehara M, Toyota K, Fukuda R, Hasegawa J, Ishida M, Nakajima T, Honda Y, Kitao O, Nakai H, Vreven T, Montgomery J A Jr, Peralta J E, Ogliaro F, Bearpark M, Heyd J J, Brothers E, Kudin K N, Staroverov V N, Kobayashi R, Normand J, Raghavachari K, Rendell A, Burant J C, Iyengar S S, Tomasi J, Cossi M, Rega N, Millam J M, Klene M, Knox, J E, Cross J B, Bakken V, Adamo C, Jaramillo J, Gomperts R, Stratmann R E, Yazyev O, Austin A J, Cammi R, Pomelli C, Ochterski J W, Martin R L, Morokuma K, Zakrzewski V G, Voth G A, Salvador P, Dannenberg J J, Dapprich S, Daniels A D, Farkas Ö, Foresman J B, Ortiz J V, Cioslowski J, Fox, D J Gaussian, Inc., Wallingford CT, 2009.
- 44 Spackman MA, McKinnon JJ (2002) Fingerprinting Intermolecular Interactions in Molecular Crystals. *Cryst Eng Comm* 4: 378-392.
- 45 Jayatilaka D, Grimwood DJ (2003) Tonto: A Fortran Based Object-Oriented System for Quantum Chemistry and Crystallography. In *Computational Science-ICCS 2660*: 142-151.
- 46 Keith TA (2013) AIMALL, version 13.05.06, TK Gristmill Software, Overland Park, KS, USA.
- 47 Bader R (1990) *Atoms in Molecules: A Quantum Theory*, International Series of Monographs on Chemistry. Clarendon Press.
- 48 Owczarek M, Majerzc I, Jakubas R (2014) Weak hydrogen and dihydrogen bonds instead of strong N-H \cdots O bonds of a tricyclic [1,2,4,5]-tetrazine derivative. Single-crystal X-ray diffraction, theoretical calculations and Hirshfeld surface analysis. *Cryst Eng Comm* 16: 7638-7648.
- 49 Spackman M A, McKinnon J J (2002) Fingerprinting intermolecular interactions in molecular crystals. *CrystEngComm* 4:378-392.
- 50 Owczarek M, Majerzc I, Jakubas R (2014) Weak hydrogen and dihydrogen bonds instead of strong N-H \cdots O bonds of a tricyclic [1,2,4,5]-tetrazine derivative. Single-crystal X-ray diffraction, theoretical calculations and Hirshfeld surface analysis *CrystEngComm*, 16: 7638-7648.